THE JOURNAL OF BIOLOGICAL CHEMISTRY VOL. 287, NO. 26, pp. 22112–22122, June 22, 2012

Ack1-mediated Androgen Receptor Phosphorylation Modulates Radiation Resistance in Castration-resistant Prostate Cancer*[S]

Received for publication, February 29, 2012, and in revised form, May 4, 2012 Published, JBC Papers in Press, May 7, 2012, DOI 10.1074/jbc.M112.357384

Kiran Mahajan[‡], Domenico Coppola[§¶], Bhupendra Rawal[‖], Y. Ann Chen[‖], Harshani R. Lawrence[‡], Robert W. Engelman[§], Nicholas J. Lawrence[‡**], and Nupam P. Mahajan[‡‡‡1]**

From the Departments of [‡]Drug Discovery, [§]Anatomic Pathology, [¶]Experimental Therapeutics, and [‖]Biostatistics and the [**]High-throughput Screening Core Facility, Moffitt Cancer Center, Tampa, Florida 33612 and [‡‡]Department of Oncologic Sciences, University of South Florida, Tampa, Florida 33620

Background: The molecular mechanisms of acquisition of radioresistance in CRPC are not fully understood.
Results: Ack1/AR signaling modulates ATM expression to promote radioresistance.
Conclusion: Ack1/AR signaling plays a critical role in acquisition of radioresistance in CRPC by modulating the DNA damage response pathways.
Significance: Ack1/AR signaling represents a new paradigm of radioresistance in CRPC that can be targeted with AIM-100.

Androgen deprivation therapy has been the standard of care in prostate cancer due to its effectiveness in initial stages. However, the disease recurs, and this recurrent cancer is referred to as castration-resistant prostate cancer (CRPC). Radiotherapy is the treatment of choice; however, in addition to androgen independence, CRPC is often resistant to radiotherapy, making radioresistant CRPC an incurable disease. The molecular mechanisms by which CRPC cells acquire radioresistance are unclear. Androgen receptor (AR)-tyrosine 267 phosphorylation by Ack1 tyrosine kinase (also known as TNK2) has emerged as an important mechanism of CRPC growth. Here, we demonstrate that pTyr^{267}-AR is recruited to the ATM (ataxia telangiectasia mutated) enhancer in an Ack1-dependent manner to up-regulate ATM expression. Mice engineered to express activated Ack1 exhibited a significant increase in pTyr^{267}-AR and ATM levels. Furthermore, primary human CRPCs with up-regulated activated Ack1 and pTyr^{267}-AR also exhibited significant increase in ATM expression. The Ack1 inhibitor AIM-100 not only inhibited Ack1 activity but also was able to suppress AR Tyr^{267} phosphorylation and its recruitment to the ATM enhancer. Notably, AIM-100 suppressed Ack1 mediated ATM expression and mitigated the growth of radioresistant CRPC tumors. Thus, our study uncovers a previously unknown mechanism of radioresistance in CRPC, which can be therapeutically reversed by a new synergistic approach that includes radiotherapy along with the suppression of Ack1/AR/ATM signaling by the Ack1 inhibitor, AIM-100.

Growth factor-stimulated receptor tyrosine kinases, *e.g.* EGF receptor and HER2, transiently but rapidly facilitate intracellular tyrosine kinase Ack1/Tnk2 activation, to transmit growth promoting signals (1–6). In addition, somatic autoactivating mutations and gene amplification have been reported to facilitate dysregulated Ack1 activation in lung, ovarian, and prostate cancers (3, 4, 6–9). In a recent gene expression profiling analysis, 60 of 157 primary human prostate tumors exhibited Ack1 mRNA up-regulation (8). Phosphorylation of Ack1 kinase at tyrosine 284, a major autophosphorylation site, correlates with progression of prostate, breast, and pancreatic cancers and inversely with patient survival (2, 6, 10, 11). Previously, we demonstrated that Ack1 phosphorylates AR[2] at tyrosine 267 in the transcriptional activation domain (2); AR mutated at tyrosine 267 failed to promote castration-resistant growth of prostate xenograft tumors, suggesting that this phosphorylation is critical for androgen-independent AR transactivation and tumor-promoting function (2). Notably, pTyr^{267}-AR and pTyr^{284}-Ack1 protein levels were found to be up-regulated significantly in human CRPC tumors but not in normal prostate samples. Furthermore, Ack1 transgenic mice displayed elevated levels of pTyr^{284}-Ack1 and develop prostatic intraepithelial neoplasia or PINs (3). Collectively, these data indicate that Ack1/AR-signaling regulates key cellular processes that facilitate CRPC growth.

AR is critical for growth and survival of prostate cancer cells (12, 13). Androgen deprivation therapy has been the standard of care in prostate cancer due to its effectiveness in initial stages. However, the disease recurs, and this recurrent cancer is referred to as castration-resistant prostate cancer or CRPC. CRPC is often resistant to radiotherapy, making radioresistant CRPC an incurable disease. The progression of prostate cancer to radioresistant CRPC stage is likely to be regulated by AR target gene expression because AR is functional despite the low levels of androgen (13–16). The molecular mechanism by which prostate cells acquire radioresistance is not fully under-

* This work was supported, in whole or in part, by National Institutes of Health Grant 1R01CA135328.
[S] This article contains supplemental Tables 1–4 and Figs. S1–S7.
[1] To whom correspondence should be addressed: Dept. of Drug Discovery, Moffitt Cancer Center, 12902 Magnolia Dr., Tampa, FL or Dept. of Oncologic Sciences, College of Medicine, University of South Florida, Tampa, FL 33612. Tel.: 813-407-4903; Fax: 813-979-7265; E-mail: nupam.mahajan@moffitt.org.

[2] The abbreviations used are: AR, androgen receptor; PIN, prostatic intraepithelial neoplasia; TMA, tissue microarray; Gy, gray; EdU, 5-ethynyl-2′-deoxyuridine; DHT, dihydrotestosterone; DSB, double strand break; KD, kinase-dead.

stood. Thus, identification of gene(s) modulated by androgen independent AR, which facilitates survival of irradiated CRPC cells is crucial to provide a better understanding of the molecular pathway(s) that confer radioresistance.

Genetic integrity is monitored by components of the DNA damage response pathways, which rapidly respond to perturbations in genetic integrity to coordinate processes that pause cell cycle to allow time for repair and evade cell death (17). The ATM (ataxia telangiectasia mutated) gene product is a major player in the DNA damage and cell cycle checkpoint signaling pathways and is vital to ensure genetic stability within cells (18–21). Although high levels of ATM expression are correlated with radioresistance, and conversely, the presence of missense mutations in the ATM gene is predictive of poor radiotherapy response and enhanced radiosensitivity (22–24), the molecular mechanisms by which cancer cells acquire increased ATM expression is not known.

To understand the molecular basis of radiation resistance of CRPC cells, we performed ChIP-on-chip analysis, which revealed the specific recruitment of $pTyr^{267}$-AR·Ack1 complex to the ATM gene enhancer. ATM mRNA and consequently protein expression is modulated by the Ack1-mediated phosphorylation of AR in prostate cancer cell lines, which is antagonized by the selective Ack1 inhibitor AIM-100. Furthermore, AIM-100 suppressed growth of radioresistant CRPC xenograft tumors by decreasing ATM expression. Thus, our data reveals for the first time the molecular basis by which the oncogenic kinase Ack1 directly modulates radiation resistance of the aggressive form of prostate cancer.

EXPERIMENTAL PROCEDURES

Cell Lines, Vectors, Antibodies, and Inhibitors—To generate luciferase reporter constructs, 2.8 kb upstream region containing the 364-bp ATM enhancer (ATM-pARE) or 2.4 kb upstream region lacking the enhancer (ATM-δpARE) were PCR-amplified and subcloned into pGL2 vector (Promega). Ack1 monoclonal Ab (A11), α-tubulin (TU-O2), phosphotyrosine, and AR monoclonal antibodies were purchased from Santa Cruz Biotechnology; anti-phospho-Ack1 (Tyr^{284}, Upstate); p53 Ser^{15}, p53 were purchased from Cell Signaling. ACAT and ATM rabbit monoclonal antibody (Tyr^{170}) were purchased from Epitomics, ATM mouse monoclonal antibody (ATM2C1) was purchased from Genetex, NPAT (BD Biosciences) FLAG monoclonal antibodies (Sigma), and KU-55933 were purchased from Selleck Chemicals. $pTyr^{267}$-AR antibodies were generated, and AIM-100 was synthesized at Moffitt Cancer Center as described previously (10). Cell culture of LNCAP and LAPC4 cell lines and generation and maintenance of caAck and kdAck cell lines has been described previously (1, 2).

Chromatin immunoprecipitation (ChIP) and ChIP-on-chip-LAPC4 (5×10^7 cells) were either untreated or treated with EGF ligand for 45 min. Cells were treated with 1% formaldehyde for 10 min, lysed, homogenized, and centrifuged. The pellet was suspended in shearing buffer and sonicated for 25 s. The soluble chromatin was incubated overnight at 4 °C with $pTyr^{267}$-AR antibody or total AR antibody and protein G-magnetic beads. The soluble chromatin was processed in the same way without immunoprecipitation and termed input DNA. The amount of immunoprecipitated DNA was determined by real time PCR. In the second step, PCR-amplified immunoprecipitated DNAs were ligated to short oligonucleotides to the ends. The PCR reactions were assembled and labeled with biotin using the NuGen FL-Ovation Biotin V2 kit. This fragmented material was hybridized to Affymetrix Human promoter 1.0R arrays following the Affymetrix procedure. The primer sequences amplifying the $pTyr^{267}$-AR binding region in ATM enhancer is shown in supplemental Table 4.

Ack1 Transgenic and Xenograft Mice—Mice breeding and colony maintenance was performed according to Institutional Animal Care and Use Committee protocols approved by University of Florida Division of Research Integrity and Compliance. LNCaP-caAck cells (2×10^6) were suspended in 100 μl of PBS and 100 μl of Matrigel (Discovery Labware, Bedford, MA) and injected subcutaneously into the flanks of male nude castrated mice. Mice were injected with AIM-100 (4 mg/kg of body weight per injection) on the seventh day post-injection of cells ($n = 8$ mice for each treatment). Five injections of AIM-100 were followed on 11th, 15th, 19th, 23rd, and 27th day. Tumor volumes were measured twice weekly using calipers. Two independent experiments were performed; a representative data set is shown.

IC_{50} (nM) Determination for AIM-100—Kinase assays were performed at Reaction Biology Corp. (Malvern, PA) using the "HotSpot" assay platform. In brief, substrates were freshly prepared, and required cofactors were added individually to each kinase reaction. Indicated kinases were added into the substrate solution followed by addition of AIM-100 (or staurosporine) in dimethyl sulfoxide into the kinase reaction mixture. [^{33}P]ATP (specific activity, 0.01μCi/μl final concentration) was added into the reaction mixture to initiate the reaction, followed by incubation of kinase reaction for 120 min at room temperature. The reactions are spotted onto P81 ion exchange paper (Whatman no. 3698-915), and filters were washed extensively in 0.1% phosphoric acid.

Tissue Microarray (TMA) Analysis—For assessment of ATM expression in human prostate cancer, immunohistochemistry was carried out on high-density TMAs ($n = 250$ cores) containing samples of different stages of disease as described previously (3, 10). For statistical assessment of ATM expression in prostate cancer, box plots were used to summarize the intensity sampling distribution at each progression stage. The Spearman rank correlation coefficient was estimated to access the relationship between ATM levels and progression stages and groups of prostate cancer. The progression stages from Benign prostatic hyperplasia, Prostatic intraepithelial neoplasia, G6, G7, G8–10, and CRPC were used for the correlation analysis. Analysis of variance (v) was performed to examine whether the ATM expression levels differ among different tumor stages. The Tukey-Kramer method was further performed to examine between which pairs of stages the expression levels are different. This post hoc procedure adjusts for pairwise comparisons and simultaneous inference. The Spearman rank correlation coefficient also was estimated to access the correlation between ATM levels and $pTyr^{267}$-AR.

TABLE 1
Enrichment analysis by GeneGo pathway maps

#	Signaling pathways	Total	*p* value	Genes from active data
1	Transcription_p53 signaling pathway	39	3.368E-03	p300, ATM, *MDM2*
2	Regulation of lipid metabolism_Regulation of lipid metabolism via LXR, NF-Y, and SREBP	38	2.023E-04	*SREBP1* precursor, *SREBP1* (nuclear), SCD, *SREBP1* (Golgi membrane)
3	ATP/ITP metabolism	122	3.512E-04	Adenosine kinase, ADSL, *POLR3A*, *AK5*, *RPA16*, *RPA39*
4	Regulation of lipid metabolism_Regulation of fatty acid synthase activity in hepatocytes	19	3.990E-04	*SREBP1* precursor, *SREBP1* (nuclear), *SREBP1* (Golgi membrane)
5	Regulation of lipid metabolism_RXR-dependent regulation of lipid metabolism via PPAR, RAR, and VDR	30	1.573E-03	PPAR-γ, CAR, SCD
6	Development_Slit-Robo signaling	30	1.573E-03	*SLIT3*, Tau (MAPT), *SLIT1*
7	Regulation of metabolism_Bile acid regulation of glucose and lipid metabolism via FXR	37	2.895E-03	*SREBP1* precursor, *SREBP1* (nuclear), SCD
8	Regulation of metabolism_Role of adiponectin in regulation of metabolism	43	4.449E-03	*SREBP1* precursor, *PPARGC1* (PGC1-α), *ACOX1*
9	Regulation of lipid metabolism_Insulin regulation of fatty acid metabolism	89	4.976E-03	*SREBP1* precursor, *SREBP1* (nuclear), SCD, *SREBP1* (Golgi membrane)
10	DNA damage_Role of SUMO in p53 regulation	17	7.525E-03	p300, *MDM2*

Immunohistochemical Staining of Xenograft Tumors—For assessment of ATM expression in xenografts, the xenograft tumors were excised, fixed, paraffin-embedded, and sectioned. Antigen retrieval was performed by heating the samples at 95 °C for 30 min in 10 mmol/liter sodium citrate (pH 6.0). After blocking with universal blocking serum (DAKO Diagnostic, Mississauga, Ontario, Canada) for 30 min, the samples were then incubated with rabbit monoclonal ATM antibody (1:300 dilution; Epitomics) at 4 °C overnight. The sections were incubated with biotin-labeled secondary and streptavidin-peroxidase for 30 min each (DAKO Diagnostic). The samples were developed with 3,39-diaminobenzidine substrate (Vector Laboratories, Burlington, Ontario, Canada) and counterstained with hematoxylin. The blue staining in Fig. 5*C* is due to hematoxylin staining. The oxidized hematoxylin colors nuclei of cells (and a few other objects, such as keratohyalin granules) blue.

Cell Cycle Analysis—LNCaP or LAPC4 cells were untreated, treated with 10 μM AIM-100 alone, with 5 Gy IR, or incubated overnight with AIM-100 followed by 5 Gy IR. IR treatment was performed with an x-ray machine (XRAD160 Precision x-ray, Bradford, CT). Cells were harvested after 16 h. Cells were stored in 100 μl of sodium citrate buffer. Cells were trypsinized in 450 μl of trypsin solution at room temperature for 10 min, incubated in 375 μl of trypsin inhibitor/RNase A (Sigma) solution for 10 min, stained with 250 μl of ice-cold propidium iodide solution for 10 min, and kept in the dark. Samples were analyzed using the FACSCalibur flowcytometer, 10,000 events were collected, and cell cycle analysis was carried out using the ModFit program.

EdU Assay—For rapid detection of DNA synthesis in proliferating cells, we used the chemical method, which is based on the incorporation of 5-ethynyl-2′-deoxyuridine (EdU) and its subsequent detection by a fluorescent azide through a Cu(I)-catalyzed [3 + 2] cycloaddition reaction ("click" chemistry) (25). Reagents are available as a kit from Invitrogen (catalog no. 350002). Cells were treated with IR or AIM-100 as described. EdU was added at a final concentration of 10 μM for 2 h, and cells were harvested. EdU-labeled cells were fixed with 4% paraformaldehyde, and cells were processed for measuring DNA synthesis as described in the Click-it- Edu Alexa Flour 488 Flow Cytometry Assay protocol (Invitrogen).

In Situ Labeling of DNA Strand Breaks—LAPC4 or LNCaP cells were treated with individually with AIM-100, γ-irradiated (15 Gy) or pretreated with AIM-100, followed by γ-irradiation, and fixed after 30 min or 5 h with 1% paraformaldehyde. DNA strand breaks were directly labeled with dUTP-FITC by using Terminal Deoxynucleotidyl transferase (Biovision catalog no. K401-60), and detected by flow cytometry as described previously (26).

RESULTS

pTyr^{267}-AR Initiates Distinct Transcriptional Program—Our earlier studies have demonstrated that Ack1-mediated AR Tyr^{267}-phosphorylation is critical for the progression of prostate cancer to CRPC stage (2). To identify novel genes modulated by pTyr^{267}-AR, we performed chromatin immunoprecipitation and tiled microarray (ChIP-on-chip) analysis. The specificity of the pTyr^{267}-AR antibody for ChIP analysis has been validated extensively and reported (10). Earlier, we have demonstrated that prostate-derived LAPC4 cells expressing wild type AR exhibit robust Ack1 activation upon EGF ligand treatment, which in turn, phosphorylates AR at Tyr^{267} (2). LAPC4 cells depleted of androgen and serum were either treated or untreated with EGF ligand, and ChIP was performed with pTyr^{267}-AR antibodies. A false discovery rate cut-off of $<$0.6 yielded 219 sequences (supplemental Table 1*a*) mostly in the enhancer regions (supplemental Table 1*b*). We compared peaks identified in this pTyr^{267}-AR ChIP-on-chip experiment with the published dihydrotestosterone (DHT) bound-AR ChIP-on-chip studies (27) and observed little overlap (supplemental Table 2). Only 10 peaks were found to be overlapping, which indicates that pTyr^{267}-AR initiates a distinct transcriptional program than DHT-bound AR.

The signaling pathways that are associated with enriched genes that correspond to pTyr^{267}-AR ChIP-on-chip binding peaks are shown in Table 1. It includes three members of the p53-dependent DNA damage signaling pathway: p300, MDM2, and ATM. pTyr^{267}-AR was bound to a 364-bp fragment, located on chromosome 11, at 2414 nucleotides upstream of the ATM gene transcription start site (supplemental Fig. S1). ATM is a critical upstream regulator of the DNA damage signaling and checkpoint pathway that maintains genetic integrity

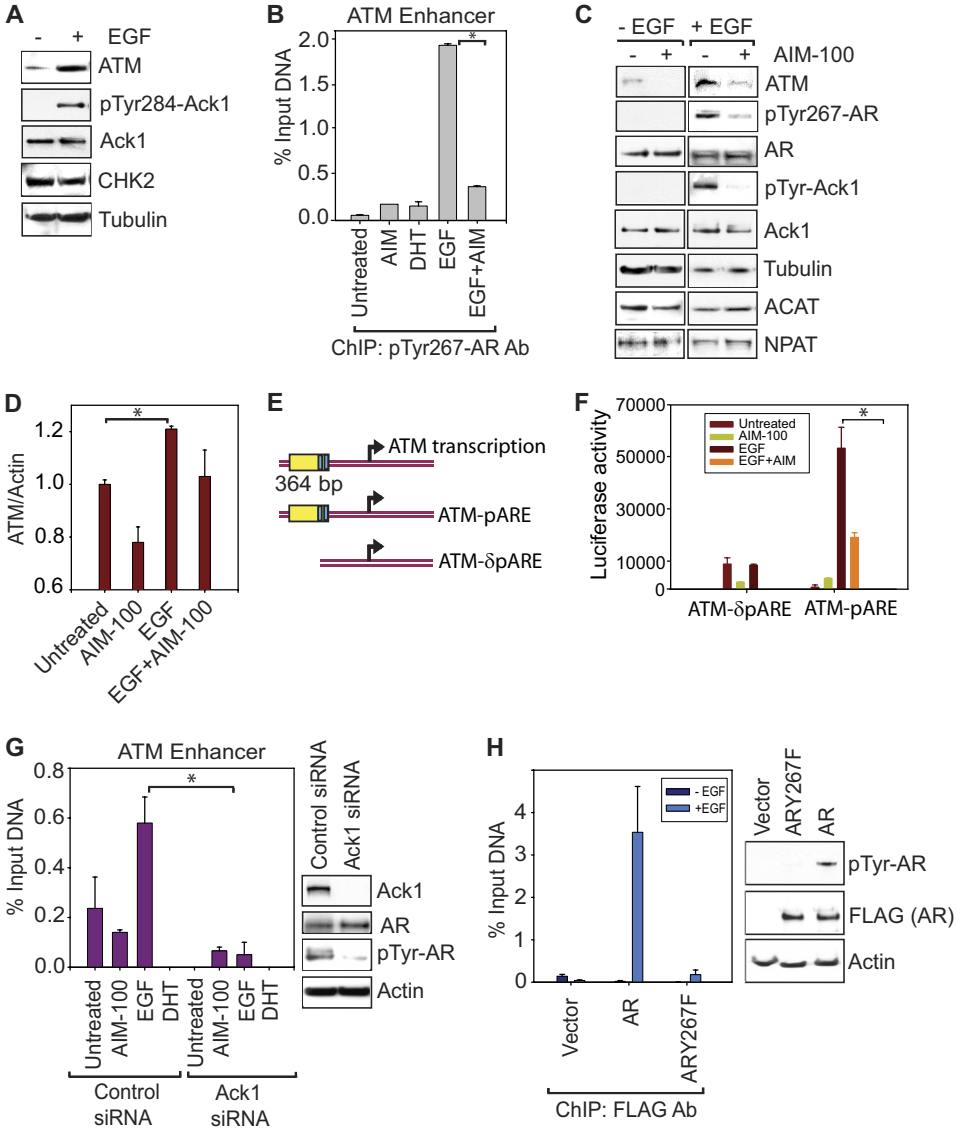

FIGURE 1. **Recruitment of the Tyr^{267}-phosphorylated AR to the ATM enhancer up-regulates ATM expression.** *A*, LAPC4 cells were either untreated or treated with EGF (10 ng/ml, 1 h). Equal amounts of whole cell extracts were analyzed by immunoblotting with the indicated antibodies (*Ab*). *B*, pTyr^{267}-AR binding to the ATM enhancer in prostate cells. Serum and androgen-depleted LAPC4 cells were either treated (or untreated) with DHT (5 nM, 16 h) or AIM-100 (1uM, 16 h) or EGF (10 ng/ml, 45 min), and EGF + AIM-100. ChIP of pTyr^{267}-AR bound to the ATM enhancer was performed, followed by quantitative PCR (*, $p = 0.013$). *C*, LAPC4 cells were both untreated or treated with AIM-100 (1 μM, 16 h), and EGF was added (10 ng/ml, 1 h). Equal amounts of whole cell extracts were analyzed by immunoblotting with indicated antibodies. *D*, LAPC4 cells were either untreated or treated with AIM-100 (2 μM, 16 h), and EGF was added (10 ng/ml, 1 h). Total RNA was extracted and analyzed by quantitative RT-PCR. Data are representative of three independent experiments (*, $p = 0.014$). *E*, the schematic of two luciferase reporter construct with the pTyr^{267}-AR binding site (ATM-pARE) and deletion construct lacking them (ATM-δpARE) are shown. *F*, LAPC4 cells were transfected with the ATM-pARE or ATM-δpARE luciferase reporter constructs (500 ng). Twenty-four hours after transfection, cells were treated with AIM-100 (10 μM) for 16 h and followed by EGF (10 ng/ml) for 3 h, and luciferase activity was determined (*, $p = 0.01$). *G*, LAPC4 cells were either transfected with control or Ack1 siRNAs followed by EGF (10 ng/ml, 45 min), AIM-100 (1 μM, 16 h), or DHT treatment. ChIP analysis for pTyr^{267}-AR binding to the ATM enhancer was performed, followed by quantitative PCR (*, $p = 0.013$). *H*, LAPC4 cells were transfected with vector (control) FLAG-tagged AR or the mutated FLAG-tagged ARY267F constructs and were either unstimulated or stimulated with EGF ligand for 45 min. ChIP was performed using FLAG antibodies followed by real time PCR for the ATM enhancer.

and facilitates DNA repair in response to DNA damage. The direct up-regulation of ATM by tyrosine phosphorylated AR has not been reported earlier and therefore provides a novel target for combating the radioresistance of prostate cancer cells by inhibiting AR/Ack1 function in cells.

To assess whether ATM is a target for Ack1/AR signaling, LAPC4 cells were treated with EGF and equal amount of the whole cell extracts were immunoblotted with ATM, pTyr-Ack1, Ack1, CHK2, and tubulin antibodies. A significant increase in pTyr^{284}-Ack1 and ATM protein levels was seen upon EGF treatment, whereas total Ack1, CHK2 and tubulin levels were unchanged (Fig. 1*A*).

AIM-100 Specifically Inhibits Ack1 Kinase Activity—To assess the role of Ack1 in pTyr^{267}-AR/ATM signaling, a Ack1-specific inhibitor is desirable. 4-amino-5,6-biaryl-furo[2,3-D]pyrimidine derivative, also known as AIM-100, has been identified as a potent inhibitor of Ack1 activity *in vitro* (10, 28). However, the kinase specificity and tumor inhibitory effect of AIM-100 was not known. To establish the specificity of AIM-100, we synthesized and determined IC_{50} values by performing

TABLE 2

IC_{50} (nM) summary table for AIM-100

NI indicates no inhibition or compound activity that could not be fit to an IC_{50} curve. Staurosporine was used as a control. LY294002 was used as control in the case of PI3Kα and -β, which is shown with an asterisk.

Kinase	AIM-100	Staurosporine
ABL1	705.90	30.25
Ack1	21.58	10.68
AKT1	NI	<1.0
AKT2	NI	<1.0
AKT3	NI	<1.0
AXL	NI	2.31
BTK	871.70	8.61
CHK1	NI	<1.0
MAP3K8	NI	>20,000
DNA-PK	NI	NI
HER2	NI	72.66
ERK1	NI	3729.00
GSK3a	NI	3.22
IGF1R	NI	10.37
IKKa	NI	76.96
IR	NI	16.91
JAK2	NI	<1.0
VEGFR2	NI	18.46
LCK	432.30	1.05
LYN	346.70	<1.0
mTOR	NI	NI
p70S6K	NI	<1.0
PDGFRa	NI	<1.0
PI3Kα	NI	667.50*
PI3Kβ	NI	362.70*
PIM1	NI	<1.0
RAF1	NI	NI
SGK1	NI	1.47
TYRO3	NI	8.00
WEE1	NI	3396.00

kinase assays in the presence of increasing concentrations of AIM-100 or with staurosporine as control (Table 2). It revealed that AIM-100 specifically inhibits Ack1 with an IC_{50} of 21 nM but not other kinases, including all the tested PI3K subfamily (to which ATM belongs) members such as ATR (ataxia telangiectasia and Rad3-related), DNA-dependent protein kinase, and mTOR (mammalian target of rapamycin).

pTyr^{267}-AR Is Recruited Specifically to ATM Enhancer—To confirm pTyr^{267}-AR binding to the ATM enhancer region, LAPC4 cells were either untreated or treated with DHT or EGF (1 h) or EGF plus AIM-100. ChIP using pTyr^{267}-AR antibodies followed by real time PCR for the ATM enhancer region revealed that pTyr^{267}-AR was recruited specifically to the ATM enhancer upon EGF stimulation (Fig. 1*B*). As a negative control, we performed ChIP using pTyr^{267}-AR and AR antibodies in DU145 cells that lack functional AR expression, which exhibited no binding to the ATM enhancer (data not shown). Consistent with the requirement for AR Tyr^{267} phosphorylation, AIM-100 treatment that specifically inhibits Ack1-mediated AR Tyr^{267} phosphorylation (Fig. 1*B*) inhibited AR recruitment to the ATM enhancer (Fig. 1*A*). To assess the effect of pTyr^{267}-AR recruitment on ATM protein expression, LAPC4 cells were either untreated or pretreated with AIM-100 alone or with AIM-100, and EGF was added. EGF-treated cells exhibited significantly higher levels of pTyr-Ack and pTyr-AR, which correlated with increased ATM levels; however, upon AIM-100 treatment, significant loss of pTyr-Ack/pTyr-AR levels and a concomitant decrease in ATM protein expression was observed (Fig. 1*C*). In contrast, protein expression of the two neighboring genes of ATM, NPAT, and ACAT were not altered (Fig. 1*C*). Consistent with LAPC4 data, LNCaP prostate cancer cells too exhibited significant decrease in ATM protein expression upon AIM-100 treatment (Supplemental Fig. S2*A*).

LAPC4 cells treated with EGF or AIM-100 followed by quantitative RT-PCR revealed up-regulated ATM mRNA levels upon EGF treatment while AIM-100 treatment abrogated this increase (Fig. 1*D*). ATM mRNA up-regulation was further confirmed in LNCaP cells stably expressing activated Ack1 or caAck (1, 2); AIM-100 treatment resulted in a significant decrease in ATM mRNA levels (supplemental Fig. S3*A*). In contrast, DHT-treated LAPC4 cells did not reveal any changes in ATM mRNA levels (supplemental Fig. S3*B*). The AR-responsive gene PSA was used as control for DHT-mediated stimulation. To determine whether pTyr^{267}-AR binding to the ATM enhancer affects the neighboring genes of ATM, relative mRNA levels of ACAT, C11ORF65, KDELC2, and NPAT were determined. Real time quantitative RT-PCR revealed that RNA levels of all four neighboring genes were not altered (supplemental Fig. S2*B*). Taken together, these data indicate Ack1 dependent pTyr^{267}-AR recruitment specifically to the ATM enhancer, which can be suppressed by AIM-100.

Characterization of Tyr^{267}-phosphorylated AR Recruitment to ATM Enhancer—The ATM gene is large, spanning ~150 kb of genomic DNA and encodes a mRNA of ~9.4 kb and a protein of 3056 amino acids or 350 kDa (29). With such a large RNA molecule, a robust increase in mRNA levels may not be apparent; however, the modest increase in mRNA levels translated into significant increase in the protein levels (Fig. 1*C*). A similar modest increase in ATM mRNA levels has been reported in the literature (30). We observed that the pTyr^{267}-AR is recruited to the 364-bp ATM enhancer sequence, which contains two ARE-like half-sites, TGTTCT (supplemental Figs. S1 and S5*A*). To further validate the pTyr^{267}-AR recruitment to the ATM enhancer, luciferase reporter constructs containing 364-bp ATM enhancer regions (ATM-pARE) or lacking it (ATM-δpARE) were constructed (Fig. 1*E*). EGF treatment of LAPC4- or heregulin-treated LNCaP cells transfected with ATM-pARE exhibited significant increase in luciferase activity, which was inhibited by AIM-100 (Fig. 1*F* and supplemental Fig. S4*A*). In contrast, DHT-treated ATM-pARE exhibited minimal luciferase activity (supplemental Fig. S5*B*). As a positive control, LAPC4 cells were transfected with AR-responsive reporter construct ARR2PB, which exhibited high luciferase activity upon DHT treatment (supplemental Fig. S5*B*). These data indicate that AR recruitment to the ATM enhancer is dependent on AR phosphorylation at Tyr^{267}.

To evaluate further the underlying mechanism of pTyr-AR binding to the ATM enhancer, we assessed the role of Ack1. Earlier, we have demonstrated that Ack1 specifically phosphorylates AR and the pTyr-Ack1·pTyr-AR complex translocates to the nucleus (2). It led us to hypothesize that Ack1 may be recruited to the ATM enhancer as a component of the pTyr^{267}-AR transcriptional complex. LAPC4 and LNCaP cells were transfected with control or Ack1 siRNAs followed by ligand and/or AIM-100 treatment. ChIP with the pTyr^{267}-AR antibodies followed by real time PCR of the ATM enhancer revealed that Ack1 knockdown resulted in significant decrease in pTyr^{267}-AR binding to the ATM enhancer (Fig. 1*G* and supplemental Fig. S4*B*). Moreover, knockdown of Ack1 lead to sig-

nificant decrease in ATM levels (supplemental Fig. S6*A*). Collectively, these data reveal that Ack1·pTyr-AR complex is recruited to the ATM enhancer and Ack1 is required for pTyr-AR mediated optimal transcriptional up-regulation of ATM gene expression.

AR Phosphorylation at Tyr^{267} Promotes Binding to ATM Enhancer and Activates Transcription—To determine whether tyrosine 267 phosphorylation of the androgen receptor is required for binding to the ATM enhancer site, vector (control), FLAG-tagged AR, or the mutant FLAG-tagged ARY267F constructs were transfected into LAPC4 prostate cell lines. These cells were either untreated or stimulated with EGF after serum starvation. ChIP was performed using FLAG antibodies followed by real time PCR for the ATM enhancer. AR bound to the ATM enhancer upon EGF stimulation. In contrast, ARY267F mutant was compromised significantly in its ability to bind to the ATM enhancer (Fig. 1*H*).

To determine the effect on ATM transcriptional activation, luciferase assay was performed. HEK293 cells that have undetectable levels of endogenous AR expression were transfected with AR or ARY267F mutant and luciferase reporter constructs containing the ATM enhancer region, ATM-pARE (shown in Fig. 1*E*). 24 h post-transfection, cells were treated with AIM-100 overnight. 48 h post-transfection, cells were treated with EGF ligand, and luciferase activity was measured. A significant increase in luciferase activity was seen in AR-transfected cells, in contrast, ARY267F mutant expressing cells exhibited minimal luciferase activity (supplemental Fig. S6*B*). Taken together, these results suggested that AR phosphorylation at Tyr^{267} promotes recruitment to the ATM enhancer and activates ATM transcription.

Probasin-Ack1 Transgenic Mice Display AR Tyr^{267} Phosphorylation and ATM Up-regulation—To determine whether up-regulation of ATM expression by pTyr-Ack1/pTyr-AR signaling occurs *in vivo*, we developed a transgenic mouse model in which Myc-tagged activated Ack1 was driven by a probasin promoter (PB-Ack) (3). These mice display a significant increase in Ack1 Tyr^{284} phosphorylation and developed mouse prostatic intraepithelial neoplasia by 44 weeks. A few older mice developed adenocarcinoma in dorsal lobe of prostate by ~50 weeks (3). The prostate lysates of PB-Ack transgenic mice were immunoblotted with pTyr^{267}-AR and ATM antibodies. In contrast to wild type littermates (WT), transgenic or transgenic mice display significant increase in AR Tyr^{267} phosphorylation and ATM up-regulation (Fig. 2, *A*, *top two panels*, and *B*). Immunohistochemical staining of PINs revealed an increase in pTyr267-AR and the ATM protein staining in transgenic mice compared with the prostates of WT mice (Fig. 2*C*).

Up-regulation of ATM Expression Correlates with Human Prostate Cancer Progression to Castration Resistance—To investigate the pTyr^{267}-AR mediated up-regulation of the ATM levels in primary human CRPCs, we performed ATM immunohistochemical analysis of TMA of clinically annotated prostate tumor samples ($n = 250$; for CRPC samples, see supplemental Table 3*A*). Generation of prostate TMA was described previously (10). A significant increase in the expression of ATM was observed when prostate cancers from progressive stages were examined (Fig. 3*A*), which was positively correlated with the

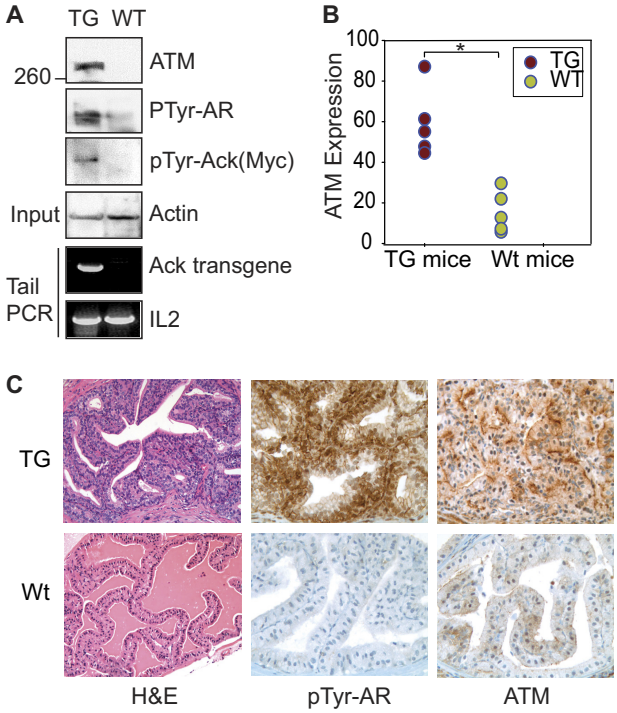

FIGURE 2. **PB-Ack1 transgenic mice display increased pTyr^{267}-AR and ATM protein expression.** *A*, 45-week-old PB-Ack1 transgenic (*TG*) mice with PIN and WT mice prostate lysates were subjected to immunoblotting using ATM monoclonal antibody (Genetex, ATM2C1) and actin antibodies (*top* and *fourth panel*, respectively). Lysates were also immunoprecipitated using anti-pTyr antibodies followed by immunoblotting with pTyr^{267}-AR antibodies (*second panel*) and anti-Myc antibodies followed by immunoblotting with Ack1 antibodies (*third panel*). *B*, ATM expression in transgenic and WT mice ($n = 5$, each) was determined using immunoblotting followed by quantification by SCION Image software. A significant increase in ATM levels in transgenic mice was seen compared with the WT mice (*, $p = 0.016$). *C*, hematoxylin and eosin (H&E) and immunohistochemical staining of WT and transgenic mice prostates. Histological appearance of the prostate lateral lobe from a WT mouse and corresponding lobe from age-matched transgenic mouse with PIN are shown (H&E staining, the *first two panels*). A significant increase in pTyr^{267}-AR (*middle panels*) and ATM (*last panels*) protein levels is observed in prostates of transgenic mice.

severity of disease progression ($r = 0.44$, $p < 0.0001$; Fig. 3*B*). Analysis of variance results indicated that ATM expression differed significantly among progression stages and CRPC ($p < 0.0001$). The results from all pair wise comparison using the Tukey-Kramer method for ATM staining between different groups are summarized in supplemental Table 3*b*. Previously, we observed increased pTyr-Ack1/pTyr-AR levels in CRPC tumors (2, 3, 10). Upon comparison, a significant positive correlation between the levels of pTyr^{267}-AR and ATM expression was observed in the prostate TMA (Spearman rank correlation coefficient $r = 0.26$, $p < 0.0001$) suggesting that prostate tumors expressing high levels of pTyr^{267}-AR are likely to have up-regulated ATM levels (Fig. 3*C*).

Ack1 Inhibitor, AIM-100, Overrides IR-induced G_2/M Checkpoint—ATM, a DNA damage sensor, rapidly activated by double strand breaks (DSBs) caused by ionizing radiation, activates signaling cascades to inhibit cell cycle progression and promote DNA repair processes (17, 31, 32). ATM is autophosphorylated at serine 1981 upon DSB induction (19) and in turn phosphorylates key checkpoint effectors such as p53 in response to DNA damage (17, 33). We tested the effect of AIM-

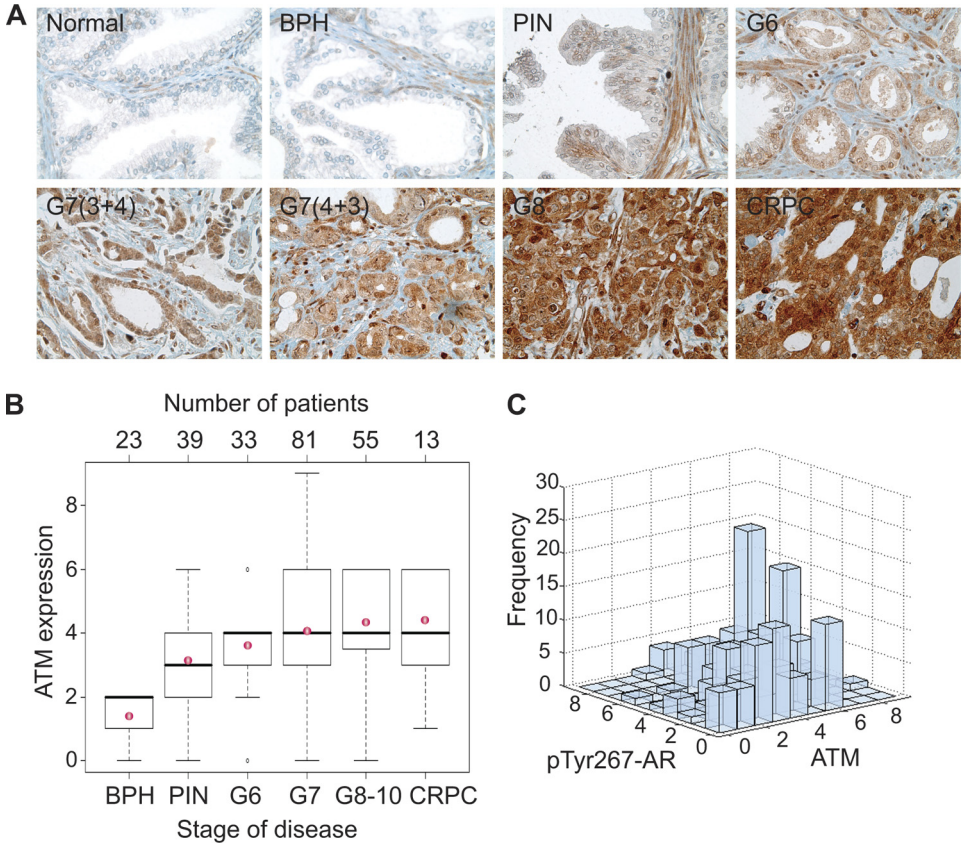

FIGURE 3. **ATM expression correlates with prostate cancer progression and pTyr^{267}-AR expression.** *A*, TMA sections representing different prostate cancer stages stained with ATM antibodies. *B*, box plots to summarize distributions of ATM staining intensities in different stages of prostate cancer. A significant increasing trend of intensity across progression stages was detected (Spearman rank correlation coefficient $r = 0.44$, $p < 0.0001$). The *box* has *lines* at the lower quartile (25%), median (50%), and upper quartile values (75%), whereas the *red circle* marks the mean value. *Whiskers* extend from each end of the *box* to the most extreme values within 1.5 times the interquartile range from the ends of the *box*. The data with values beyond the *ends* of the *whiskers*, displayed with *black circles*, are potential outliers. *C*, expression levels of Tyr^{267}-phosphorylated AR and ATM were significantly correlated in prostate tumors (Spearman rank correlation coefficient = 0.26, $p < 0.0001$).

100 on the DNA repair and checkpoint functions of ATM in response to IR-induced DNA damage. IR+AIM-100-treated cells exhibited loss of ATM Ser^{1981} phosphorylation and loss of ATM substrate phosphorylation, p53 at Ser^{15} (Fig. 4*A*), suggesting that by inhibiting ATM expression, AIM-100 suppresses ATM autoactivation and ATM-mediated activation of other cell cycle effectors. Furthermore, cell cycle analysis was performed on cells that were irradiated in the presence and absence of the Ack inhibitor. The majority of the untreated cells were in the G_1/S phase of the cell cycle; however, upon IR treatment, a substantial increase in the number of cells in G_2 phase (84%) was observed, indicative of G_2/M arrest. When cells were treated with both AIM-100 and IR, the proportion of cells in G_2 phase was decreased significantly (84 to 38%), indicating the loss of G_2 arrest (Fig. 4*B*).

To assess whether IR+AIM-100-treated cells had unrepaired DSBs, DSB quantitation assay was performed as described previously (26). IR treatment alone caused DSBs, which were repaired in 5 h, as seen by significant decrease in FITC-positive cells (Fig. 4, *C* and *D*). In contrast, the number of cells with DSBs remained high even after 5 h of post-IR incubation in IR+AIM-100-treated cells, suggesting compromised DNA repair ability of these cells that failed to arrest due to the loss of G_2 arrest (Fig. 4, *C* and *D*). As a control, the cells were pretreated with ATM inhibitor KU-55933 followed by IR (34). Irradiated prostate cancer cells treated with the ATM inhibitor also showed a similar decrease in the number of cells in G_2 as seen with AIM-100 (Fig. 4*E*). Thus, similar outcomes in both the inhibitor treatments suggest that AIM-100 inhibits IR induced ATM G_2/M checkpoint activity.

Inhibition of Ack1/pTyr-AR Radiosensitizes CRPC Tumor Growth—Activation of the DNA damage checkpoints in response to DSBs is known to promote radioresistance (35, 36). To assess whether preferential up-regulation of ATM expression by pTyr^{267}-AR may confer radioresistance, we used LNCaP cells that are stably transfected with activated Ack1 (LNCaP-caAck cells) (1). LNCaP-caAck cells exhibit AR Tyr^{267}-phosphorylation and promote castration-resistant growth of xenograft tumors (2). To assess the radiosensitivity, clonogenic assay was performed, which revealed that in contrast to LNCaP cells, LNCaP-caAck cells formed a significantly higher number of colonies at high doses of radiation (Fig. 5*A* and supplemental Fig. S7*A*). Unirradiated or irradiated LNCaP-caAck cells were injected in castrated nude mice. One week after injection when palpable tumors were noticed, AIM-100 was injected, and tumor growth was monitored. Unirradiated LNCaP-caAck cells formed robust xenograft tumors, which showed ~50% decrease upon AIM-100 treatment (Fig. 5*B*).

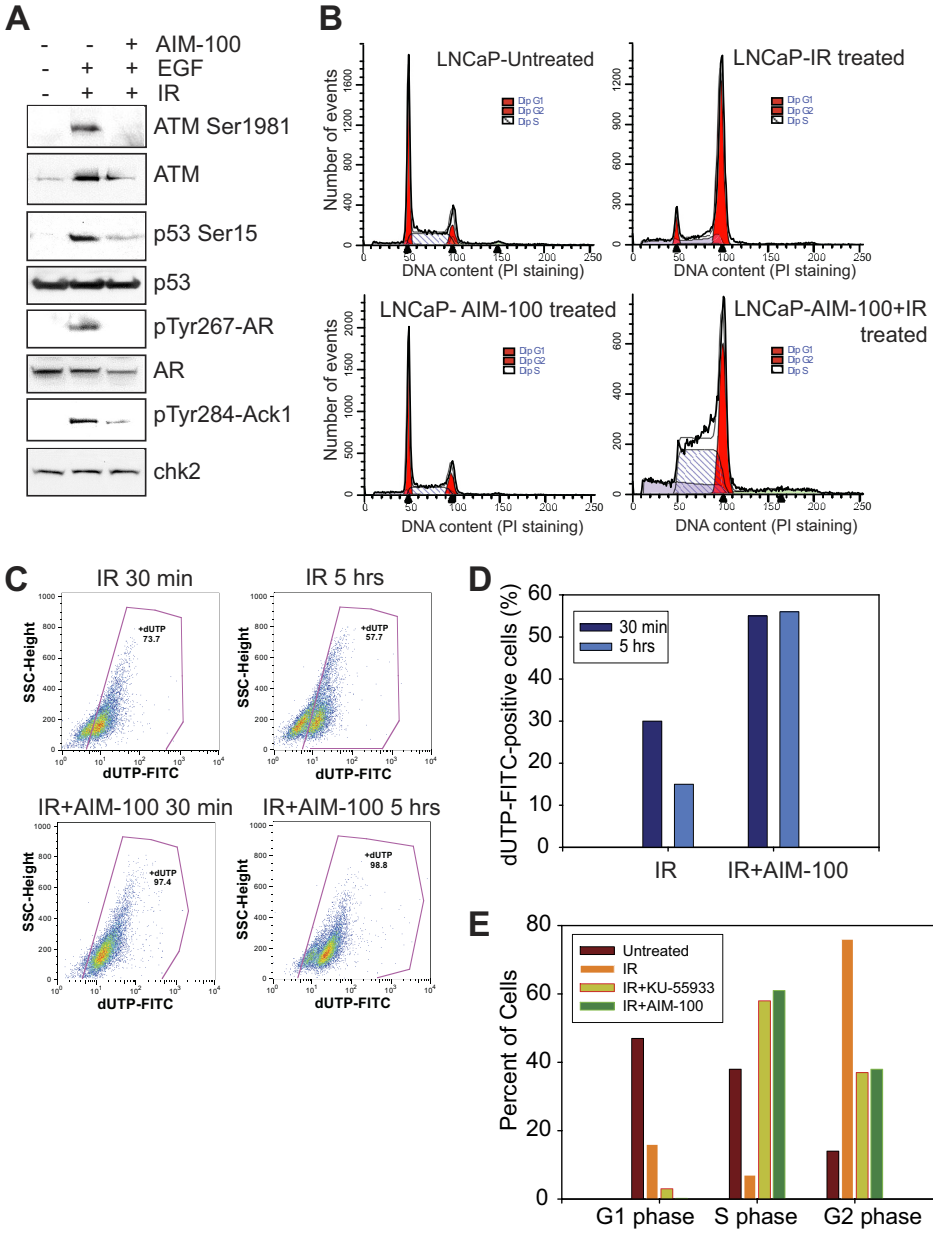

FIGURE 4. **AIM-100 suppresses ATM-mediated cell cycle checkpoint and DNA repair in irradiated prostate cells.** *A*, LAPC4 cells were treated with IR (10 Gy) and IR+AIM-100 (1 μM, 24 h). Equal amounts of whole cell extracts analyzed by immunoblotting with indicated antibodies. *B*, cell cycle analysis by flow cytometry. LNCaP cells were untreated or treated with IR (5 Gy) or AIM-100 (5 μM, 24 h) or IR and AIM-100. Cells were stained with propidium iodide, and DNA content was measured. 20,000 cells were measured by flow cytometry. Three independent experiments were performed, and a representative data set is shown. *C*, LNCaP cells were treated with IR (15 Gy) and IR+AIM-100 (5 μM), and the number of DSBs was measured by labeling DNA ends with FITC-dUTP in the presence of TdT polymerase. 20,000 events were collected by flow cytometry, and FITC-positive cells are shown. Three independent experiments were performed; a representative data set is shown. *D*, histogram representing number of cells is shown. A fraction of cells (42.6%), which stained positive in AIM-100 treatment alone, are dying cells. These were considered as base-line and were deducted from all IR-treated samples. *E*, cell cycle analysis by flow cytometry. LNCaP cells were untreated or treated with IR (5 Gy) or IR and AIM-100 or KU55933 (10 μM, 24 h). Cells were stained with propidium iodide, and DNA content was measured. The experiment was performed in triplicate, and a representative data set is shown.

Notably, the irradiated LNCaP-caAck cells too formed tumors; however, their growth was significantly suppressed on injection with AIM-100 (Fig. 5*B*). We assessed the body weight of the dimethyl sulfoxide and AIM-100-injected castrated nude mice during the course of the experiment and did not observe any morbidity or statistically significant differences in the body weight of the two groups (supplemental Fig. S7*B*). The CRPC xenografts were excised and stained with the ATM antibodies, revealing high levels of ATM in dimethyl sulfoxide-injected xenografts before and after irradiation; however, upon treatment with AIM-100, ATM levels were significantly down-regulated (Fig. 5*C*). Furthermore, a significant necrosis in AIM-100-treated mice xenografts was observed (H&E stained *lower panel*, Fig. 5*C*), which explains the significant decrease in the tumor volume that was seen in Fig. 5*B*.

ATM, Primary Target of pTyr-Ack1/pTyr-AR Signaling—To validate that ATM is the main target of the action of AIM-100, we performed the "rescue" experiment. We observed that irradiated LNCaP-caAck xenografts injected with AIM-100 exhibited minimal tumor growth (Fig. 5*B*), suggesting that AIM-100-

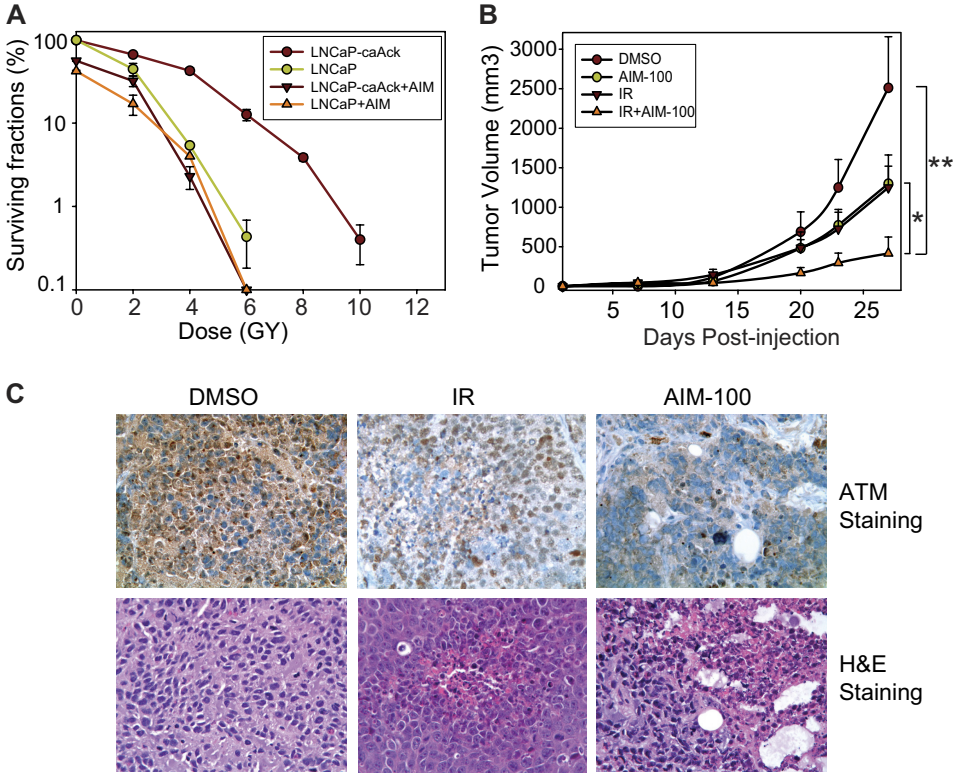

FIGURE 5. **Enhanced radiosensitization of castration-resistant prostate cells treated with AIM-100.** *A*, clonogenic survival assay. LNCaP and LNCaP-caAck cells (1000 cells/10 cm plate) were irradiated 0–10 Gy and plated. The colonies were fixed, stained, and counted (*, $p < 0.01$). *B*, castrated nude male mice were injected with unirradiated or irradiated (1.5 Gy) LNCaP-caAck-expressing cells. Mice were injected with AIM-100 (4 mg/kg of body weight per injection) on seventh day post-injection of cells ($n = 8$ mice for each treatment). Five injections of AIM-100 were followed on 11th, 15th, 19th, 23rd, and 27th day. Tumor volumes were measured; *, $p = 0.024$; **, $p = 0.041$. Two independent experiments were performed; a representative data set is shown. *C*, immunohistochemical (*upper panels*) and H&E (*lower panels*) staining of irradiated LNCaP-caAck xenograft tumors excised from dimethyl sulfoxide (*left panels*; *DMSO*) or AIM-100 (*right panels*) injected mice. The *blue* staining in *C* is due to hematoxylin stain.

mediated suppression of ATM expression resulted in a failure to repair of DSBs and thus the susceptibility to irradiation. We hypothesized that expression of ATM from promoter that is not regulated by pTyr^{267}-AR might allow irradiated LNCaP-caAck xenografts to grow in the presence of AIM-100. LNCaP-caAck cells were transfected with FLAG-tagged kinase-dead (KD)-ATM or wild type (WT)-ATM expressing constructs that are regulated by CMV promoter (Fig. 6*A*). Cells were irradiated and injected in castrated mice, and later, the mice were injected with AIM-100. The KD-ATM-expressing cells exhibited minimal tumor growth; however, Wt-ATM expressing cells exhibited significant tumor growth (Fig. 6*B*), indicating that AIM-100-mediated inhibition of Ack1/pTyr-AR/ATM signaling is mainly responsible for the radiosensitization of xenografts.

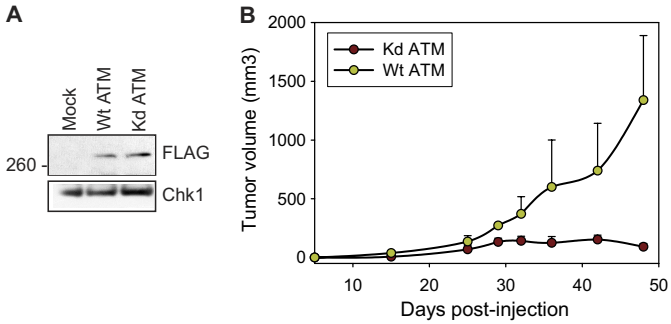

FIGURE 6. **Ack1/AR signaling modulates ATM expression.** *A*, LNCaP-caAck cells were transfected with FLAG-tagged KD-ATM or WT-ATM expressing constructs followed by immunoblotting with FLAG antibodies. *B*, castrated nude male mice were injected with irradiated (1.5 Gy) LNCaP-caAck cells expressing KD-ATM or WT-ATM. Mice were injected with AIM-100 (4 mg/kg of body weight per injection) on 12th day post-injection of cells ($n = 5$ mice for each treatment). Four injections of AIM-100 were followed on 15th, 19th, 23rd, and 27th day. Tumor volumes were measured.

DISCUSSION

Our studies collectively demonstrate a novel mechanism in which Ack-induced phosphorylation of AR up-regulates the expression of ATM in prostate cancer cells. ATM is a critical regulator of the DNA damage checkpoint response pathways, which ensures genetic integrity and cell survival. Checkpoint genes ensure genetic integrity by arresting the cell cycle to facilitate repair. In the absence of repair, these cells can undergo apoptosis or cell senescence or subvert checkpoints to have pathological consequences by resuming the cell cycle progression upon checkpoint termination (37). Thus, up-regulation and activation of the DNA damage checkpoint protein, ATM, in irradiated prostate cancer cells is likely to increase the DNA repair capacity and facilitate recovery of cells, underlying tumor radioresistance (38). Consistent with our observation, previous studies demonstrate that the glioma stems cells display preferential activation of the DNA damage checkpoint response pathways resulting in increased radioresistance in malignant brain cancer (35).

Radiation therapy is the primary treatment of choice for localized prostate cancer. However, resistance to ionizing radi-

ation remains a major obstacle in CRPC therapy. Therefore, inhibitors of the DNA damage checkpoint pathway such as ATM, CHK1, and CHK2 inhibitors, that radiosensitize tumor cells and potentiate cytotoxicity are promising chemotherapeutic options (34, 39, 40). However, because they can also compromise repair of damaged DNA of the neighboring normal tissues their use is limited. Thus, inhibitors targeting the signaling pathways that confer radioresistance in specific tissues such as the prostate are urgently needed. Currently, limited therapeutic options are available for men with CRPC, and thus the treatment of CRPC remains a challenging proposition as most of the agents have been modestly effective against the CRPC (41). Our data has uncovered a new signaling mechanism that indicates ATM up-regulation due to the activation of Ack1/AR signaling in CRPC. Cells expressing activated Ack1 are significantly radioresistant as seen in clonogenic survival assays and in their ability to form xenograft tumors even after irradiation (Fig. 5, *A* and *B*). Treatment of the radioresistant CRPC cells with AIM-100 suppressed ATM expression, which was reflected in a failure of the CRPC cells to repair the DSBs upon irradiation (Figs. 4 and 5). Consistent with these data, combination of AIM-100 treatment with irradiation resulted in radiosensitization of the CRPC cells, leading to suppression of castration resistant xenograft tumors in mice (Fig. 5*B*). Thus, Ack1 inhibitors are likely to selectively radiosensitize prostate cancer tissues that are dependent on AR for their growth without affecting other tissues that lack AR expression.

In summary, our work identifies a signaling nexus consisting of three key players ATM, a DNA damage-dependent kinase, Ack1, a growth factor regulated tyrosine kinase, and steroid receptor AR that play a crucial role in radioresistance of hormonally insensitive prostate cancer. The cross-talk between them defines a previously unknown mechanism by which metastatic prostate cancer cells survive IR-induced killing. Consequently, inhibition of the signaling by synergistic approach that includes both radiotherapy and chemotherapy with selective Ack1 inhibitors opens up a novel therapeutic option for CRPC patients.

Acknowledgments—We thank Dr. Michael Kastan for ATM expression constructs, Drs. Ed Seto and Alvaro Monteiro for insightful suggestions, Xiaotao Qu for bioinformatics analysis of ChIP-on-chip data, Laura Hall for real time PCR, and Holly Barber for mice breeding and maintenance.

REFERENCES

1. Mahajan, N. P., Whang, Y. E., Mohler, J. L., and Earp, H. S. (2005) Activated tyrosine kinase Ack1 promotes prostate tumorigenesis: Role of Ack1 in polyubiquitination of tumor suppressor Wwox. *Cancer Res.* **65,** 10514–10523
2. Mahajan, N. P., Liu, Y., Majumder, S., Warren, M. R., Parker, C. E., Mohler, J. L., Earp, H. S., and Whang, Y. E. (2007) Activated Cdc42-associated kinase Ack1 promotes prostate cancer progression via androgen receptor tyrosine phosphorylation. *Proc. Natl. Acad. Sci. U.S.A.* **104,** 8438–8443
3. Mahajan, K., Coppola, D., Challa, S., Fang, B., Chen, Y. A., Zhu, W., Lopez, A. S., Koomen, J., Engelman, R. W., Rivera, C., Muraoka-Cook, R. S., Cheng, J. Q., Schönbrunn, E., Sebti, S. M., Earp, H. S., and Mahajan, N. P. (2010) Ack1 mediated AKT/PKB tyrosine 176 phosphorylation regulates its activation. *PLoS One* **5,** e9646
4. Mahajan, K., and Mahajan, N. P. (2010) Shepherding AKT and androgen receptor by Ack1 tyrosine kinase. *J. Cell Physiol.* **224,** 327–333
5. Mahajan, K., and Mahajan, N. P. (February 3, 2012) *J. Cell. Physiol.*, 10.1002/jcp.24065. [Epub ahead of print]
6. Mahajan, K., Coppola, D., Chen, Y. A., Zhu, W., Lawrence, H. R., Lawrence, N. J., and Mahajan, N. P. (2012) Ack1 tyrosine kinase activation correlates with pancreatic cancer progression. *Am. J. Pathol.* **180,** 1386–1393
7. van der Horst, E. H., Degenhardt, Y. Y., Strelow, A., Slavin, A., Chinn, L., Orf, J., Rong, M., Li, S., See, L. H., Nguyen, K. Q., Hoey, T., Wesche, H., and Powers, S. (2005) Metastatic properties and genomic amplification of the tyrosine kinase gene ACK1. *Proc. Natl. Acad. Sci. U.S.A.* **102,** 15901–15906
8. Taylor, B. S., Schultz, N., Hieronymus, H., Gopalan, A., Xiao, Y., Carver, B. S., Arora, V. K., Kaushik, P., Cerami, E., Reva, B., Antipin, Y., Mitsiades, N., Landers, T., Dolgalev, I., Major, J. E., Wilson, M., Socci, N. D., Lash, A. E., Heguy, A., Eastham, J. A., Scher, H. I., Reuter, V. E., Scardino, P. T., Sander, C., Sawyers, C. L., and Gerald, W. L. (2010) Integrative genomic profiling of human prostate cancer. *Cancer Cell* **18,** 11–22
9. Prieto-Echagüe, V., Gucwa, A., Craddock, B. P., Brown, D. A., and Miller, W. T. (2010) Cancer-associated mutations activate the nonreceptor tyrosine kinase Ack1. *J. Biol. Chem.* **285,** 10605–10615
10. Mahajan, K., Challa, S., Coppola, D., Lawrence, H., Luo, Y., Gevariya, H., Zhu, W., Chen, Y. A., Lawrence, N. J., and Mahajan, N. P. (2010) Effect of Ack1 tyrosine kinase inhibitor on ligand-independent androgen receptor activity. *Prostate* **70,** 1274–1285
11. Yokoyama, N., and Miller, W. T. (2003) Biochemical properties of the Cdc42-associated tyrosine kinase ACK1. Substrate specificity, authphosphorylation, and interaction with Hck. *J. Biol. Chem.* **278,** 47713–47723
12. Litvinov, I. V., De Marzo, A. M., and Isaacs, J. T. (2003) Is the Achilles' heel for prostate cancer therapy a gain of function in androgen receptor signaling? *J. Clin. Endocrinol. Metab.* **88,** 2972–2982
13. Chen, Y., Sawyers, C. L., and Scher, H. I. (2008) Targeting the androgen receptor pathway in prostate cancer. *Cur. Opin. Pharmacol.* **8,** 440–448
14. Attar, R. M., Takimoto, C. H., and Gottardis, M. M. (2009) Castration-resistant prostate cancer: Locking up the molecular escape routes. *Clin. Cancer Res.* **15,** 3251–3255
15. Chen, C. D., Welsbie, D. S., Tran, C., Baek, S. H., Chen, R., Vessella, R., Rosenfeld, M. G., and Sawyers, C. L. (2004) Molecular determinants of resistance to antiandrogen therapy. *Nat. Med.* **10,** 33–39
16. Waltering, K. K., Helenius, M. A., Sahu, B., Manni, V., Linja, M. J., Jänne, O. A., and Visakorpi, T. (2009) Increased expression of androgen receptor sensitizes prostate cancer cells to low levels of androgens. *Cancer Res.* **69,** 8141–8149
17. Jackson, S. P., and Bartek, J. (2009) The DNA-damage response in human biology and disease. *Nature* **461,** 1071–1078
18. Kastan, M. B. (2008) DNA damage responses: Mechanisms and roles in human disease: 2007 G.H.A. Clowes Memorial Award Lecture. *Mol. Cancer Res.* **6,** 517–524
19. Bakkenist, C. J., and Kastan, M. B. (2003) DNA damage activates ATM through intermolecular autophosphorylation and dimer dissociation. *Nature* **421,** 499–506
20. Shiloh, Y. (2003) ATM and related protein kinases: Safeguarding genome integrity. *Nat. Rev. Cancer* **3,** 155–168
21. Matsuoka, S., Ballif, B. A., Smogorzewska, A., McDonald, E. R., 3rd, Hurov, K. E., Luo, J., Bakalarski, C. E., Zhao, Z., Solimini, N., Lerenthal, Y., Shiloh, Y., Gygi, S. P., and Elledge, S. J. (2007) ATM and ATR substrate analysis reveals extensive protein networks responsive to DNA damage. *Science* **316,** 1160–1166
22. Fang, Z., Kozlov, S., McKay, M. J., Woods, R., Birrell, G., Sprung, C. N., Murrell, D. F., Wangoo, K., Teng, L., Kearsley, J. H., Lavin, M. F., Graham, P. H., and Clarke, R. A. (2010) Low levels of ATM in breast cancer patients with clinical radiosensitivity. *Genome Integr.* **1,** 9
23. Cesaretti, J. A., Stock, R. G., Lehrer, S., Atencio, D. A., Bernstein, J. L., Stone, N. N., Wallenstein, S., Green, S., Loeb, K., Kollmeier, M., Smith, M., and Rosenstein, B. S. (2005) ATM sequence variants are predictive of adverse radiotherapy response among patients treated for prostate cancer. *Int. J. Radiat. Oncol. Biol. Phys.* **61,** 196–202

24. Pugh, T. J., Keyes, M., Barclay, L., Delaney, A., Krzywinski, M., Thomas, D., Novik, K., Yang, C., Agranovich, A., McKenzie, M., Morris, W. J., Olive, P. L., Marra, M. A., and Moore, R. A. (2009) Sequence variant discovery in DNA repair genes from radiosensitive and radiotolerant prostate brachytherapy patients. *Clin. Cancer Res.* **15,** 5008–5016
25. Salic, A., and Mitchison, T. J. (2008) A chemical method for fast and sensitive detection of DNA synthesis in vivo. *Proc. Natl. Acad. Sci. U.S.A.* **105,** 2415–2420
26. Mahajan, K. N., and Mitchell, B. S. (2003) Role of human Pso4 in mammalian DNA repair and association with terminal deoxynucleotidyl transferase. *Proc. Natl. Acad. Sci. U.S.A.* **100,** 10746–10751
27. Wang, Q., Li, W., Zhang, Y., Yuan, X., Xu, K., Yu, J., Chen, Z., Beroukhim, R., Wang, H., Lupien, M., Wu, T., Regan, M. M., Meyer, C. A., Carroll, J. S., Manrai, A. K., Jänne, O. A., Balk, S. P., Mehra, R., Han, B., Chinnaiyan, A. M., Rubin, M. A., True, L., Fiorentino, M., Fiore, C., Loda, M., Kantoff, P. W., Liu, X. S., and Brown, M. (2009) Androgen receptor regulates a distinct transcription program in androgen-independent prostate cancer. *Cell* **138,** 245–256
28. DiMauro, E. F., Newcomb, J., Nunes, J. J., Bemis, J. E., Boucher, C., Buchanan, J. L., Buckner, W. H., Cheng, A., Faust, T., Hsieh, F., Huang, X., Lee, J. H., Marshall, T. L., Martin, M. W., McGowan, D. C., Schneider, S., Turci, S. M., White, R. D., and Zhu, X. (2007) Discovery of 4-amino-5,6-biaryl-furo[2,3-D[rsqb]pyrimidines as inhibitors of Lck: Development of an expedient and divergent synthetic route and preliminary SAR. *Bioorg. Med. Chem. Lett.* **17,** 2305–2309
29. Savitsky, K., Bar-Shira, A., Gilad, S., Rotman, G., Ziv, Y., Vanagaite, L., Tagle, D. A., Smith, S., Uziel, T., Sfez, S., Ashkenazi, M., Pecker, I., Frydman, M., Harnik, R., Patanjali, S. R., Simmons, A., Clines, G. A., Sartiel, A., Gatti, R. A., Chessa, L., Sanal, O., Lavin, M. F., Jaspers, N. G., Taylor, A. M., Arlett, C. F., Miki, T., Weissman, S. M., Lovett, M., Collins, F. S., and Shiloh, Y. (1995) A single ataxia telangiectasia gene with a product similar to PI-3 kinase. *Science* **268,** 1749–1753
30. Berkovich, E., and Ginsberg, D. (2003) ATM is a target for positive regulation by E2F-1. *Oncogene* **22,** 161–167
31. Kastan, M. B., Lim, D. S., Kim, S. T., and Yang, D. (2001) ATM- a key determinant of multiple cellular responses to irradiation. *Acta Oncologica* **40,** 686–688
32. Lee, J. H., and Paull, T. T. (2007) Activation and regulation of ATM kinase activity in response to DNA double-strand breaks. *Oncogene* **26,** 7741–7748
33. Lee, J. H., and Paull, T. T. (2005) ATM activation by DNA double-strand breaks through the Mre11-Rad50-Nbs1 complex. *Science* **308,** 551–554
34. Hickson, I., Zhao, Y., Richardson, C. J., Green, S. J., Martin, N. M., Orr, A. I., Reaper, P. M., Jackson, S. P., Curtin, N. J., and Smith, G. C. (2004) Identification and characterization of a novel and specific inhibitor of the ataxia telangiectasia-mutated kinase ATM. *Cancer Res.* **64,** 9152–9159
35. Bao, S., Wu, Q., McLendon, R. E., Hao, Y., Shi, Q., Hjelmeland, A. B., Dewhirst, M. W., Bigner, D. D., and Rich, J. N. (2006) Glioma stem cells promote radioresistance by preferential activation of the DNA damage response. *Nature* **444,** 756–760
36. Cheng, L., Wu, Q., Huang, Z., Guryanova, O. A., Huang, Q., Shou, W., Rich, J. N., and Bao, S. (2011) L1CAM regulates DNA damage checkpoint response of glioblastoma stem cells through NBS1. *EMBO J.* **30,** 800–813
37. Bartek, J., and Lukas, J. (2007) DNA damage checkpoints: From initiation to recovery or adaptation. *Curr. Opin. Cell Biol.* **19,** 238–245
38. Krempler, A., Deckbar, D., Jeggo, P. A., and Löbrich, M. (2007) An imperfect G_2M checkpoint contributes to chromosome instability following irradiation of S and G_2 phase cells. *Cell Cycle* **6,** 1682–1686
39. Rainey, M. D., Charlton, M. E., Stanton, R. V., and Kastan, M. B. (2008) Transient inhibition of ATM kinase is sufficient to enhance cellular sensitivity to ionizing radiation. *Cancer Res.* **68,** 7466–7474
40. Kawabe, T. (2004) G_2 checkpoint abrogators as anticancer drugs. *Mol. Cancer Ther.* **3,** 513–519
41. Di Lorenzo, G., Buonerba, C., Autorino, R., De Placido, S., and Sternberg, C. N. (2010) Castration-resistant prostate cancer: Current and emerging treatment strategies. *Drugs* **70,** 983–1000